

Proposal for

# A Silicon Tracker for the Crystal Collimator Experiment in the H8 beam of the SPS in September 2006

*Participants: G. Ambrosi, S. Ascani, P. Azzarello,  
R. Battiston, B. Bertucci, W.J. Burger, M. Ionica,  
V. Postolache, and P. Zuccon*

*17 mai 2006*

## Introduction

A tracker composed of silicon microstrip detectors is used to measure the deflection angle produced by a bent crystal in a 400 GeV/c proton beam in the H8 line of the CERN SPS. The deflection, or scattering angle, is obtained from the particle trajectories reconstructed before and after the crystal position. Two scenarios were evaluated: upstream and downstream tracker positions compatible with the current H8 beam line configuration, and a measurement with only the downstream tracker present. The capability to measure the H8 *micro-beam* divergence with the silicon detectors was also evaluated.

## Tracker Configuration

Figure 1 shows the two-tracker configuration in the H8 beam line of the SPS West Area hall. The upstream tracker group provides a measurement of the incident beam direction over a distance of  $\sim 4.1$  m (S1, S2, and S3) and the first point on the track downstream of the bent crystal (S4). The latter, combined with the downstream telescope (S5-S8), will measure the deflected beam direction over a distance of 35 or 55 m.

The large distances between the detector locations require at least two Tracker Data Reduction (TDR) crates, where the analog-to-digital conversion of the silicon signals is performed. The maximal distance possible between

detectors of the same readout group is 6 m. The eight silicon microstrip detectors are divided into two readout groups which are managed by a common PC. The communication between readout crates and PC is provided by the *AMS-Wire* protocol, which must be verified for distances exceeding 10 m.

The upstream tracker region is shown in fig. 2. A minimal configuration would consist of two detectors separated by a distance of 4.1 m before the crystal and the detector S4. Since each TDR is capable to read two AMS-02 detectors, a third measurement point of the incident track can be accommodated.

Figure 3 shows the downstream tracker region. With at least three detectors, the position resolution can be measured, and with two TDRs, a four plane telescope (S5-S8) offers the possibility to perform a “parasite” measurement in the H8 beam.

## Expected Performance

The “geometrical” error of the angle ( $\Theta$ ) measurement, neglecting multiple scattering, is

$$\delta\Theta = \frac{\sqrt{2} \cdot \sigma}{l},$$

where  $l$  is the distance between the measurement points and  $\sigma$  the position measurement resolution. Given the inter-detector distances, the angular resolution of the upstream tracker is dependent on both the position resolution of the detectors ( $\delta\Theta \sim 5 \mu\text{rad}$ ) and multiple scattering, whereas the angular resolution of the downstream tracker ( $\delta\Theta \sim 0.5 \mu\text{rad}$ ) is dominated by the latter. An increase in the flight path from 35 to 55 m (in vacuum) does not affect the angular resolution of the downstream tracker.

A Geant simulation has been used to estimate the performance of the upstream and downstream silicon trackers for the configuration depicted in figs. 1-3. The silicon detectors S1 and S2 are located 4.4 m upstream of the position of the bent crystal; the detectors S3 and S4 are located 30 cm upstream and downstream of the crystal; and the downstream telescope (S5-S8) is placed at a distance of 35 m from the crystal. A  $180 \mu\text{m}$  thick mylar window is present at each vacuum-air interface.

In the study, the angular divergence of the beam (400 GeV/c protons) is defined as  $p_x/p_z$ , where  $x$  is the horizontal (deflection) direction and  $z$  is

the beam direction. The silicon detectors (type AMS-02) are  $7.0(x) \times 4.0(y) \times 0.03(z)$  cm<sup>3</sup> wafers with  $15 \mu\text{m}$  resolution in the  $x$  direction. The “amorphous” crystal is a  $3.0(x) \times 5.5(y) \times 0.1(z)$  cm<sup>3</sup> silicon wafer. The incident beam is generated in the first vacuum section with a  $1.8 \mu\text{rad}$  (rms) dispersion in the horizontal plane resulting in the quoted  $3 \mu\text{rad}$  (rms) dispersion of the H8 *micro-beam* at the crystal position (fig. 4).

The angular resolution for the incident beam ( $\Delta\Theta_{\text{inc}}$ ) is  $6.1 \mu\text{rad}$  (rms) for the minimal setup consisting of two detectors S1 and S3. The resolution is defined as the difference between the beam direction obtained with the two point fit and the actual angle at the entry of the crystal. The dispersion of the beam at the latter is  $4.0 \mu\text{rad}$  (rms). In comparison, the presence of three detectors in the upstream tracker results in an angular resolution of  $5.5 \mu\text{rad}$  (rms) and a beam dispersion of  $4.4 \mu\text{rad}$  (rms) at the crystal. The distributions are shown in fig. 5.

Figure 6 shows the beam distribution at the exit of the crystal and the angular resolution obtained with S4 and different combinations of S5-S8. The resolution for the emergent beam ( $\Delta\Theta_{\text{exit}}$ ) is  $2.5 \mu\text{rad}$  (rms). The scattering angle resolutions ( $\Delta\Theta_{\text{scat}}$ ) are  $6.6$  and  $6.0 \mu\text{rad}$  (rms) respectively for the two and three detector configurations of the upstream tracker (fig. 7).

The position resolution of the upstream tracker may be improved by replacing the AMS-02 detectors with smaller,  $1.9 \times 1.9$  cm<sup>2</sup>, silicon detectors from IRST; with a  $50 \mu\text{m}$  readout pitch, a factor of two improvement in the position resolution is expected ( $7.5 \mu\text{m}$ ). The results obtained with the IRST detectors are also shown in figs. 5-7.

The results are summarized in table 1. The dispersion of the H8 *micro-beam* is smaller than the measurement resolution of the incident beam provided by the AMS-02 detectors. In terms of resolution, only an upstream silicon tracker equipped with the better resolution IRST detectors appears viable. In this case, the scattering angle resolutions are comparable:  $4.4 \mu\text{rad}$  (rms) for the two-tracker configuration and  $4.0 \mu\text{rad}$  (rms) with the  $3.0 \mu\text{rad}$  (rms) *micro-beam* and the downstream tracker (fig. 7). In addition, an upstream telescope equipped with the IRST detectors would determine the position at the crystal of the incident proton with a precision of  $8 \mu\text{m}$  (fig. 8). The presence of the better resolution detectors in the downstream tracker has a negligible effect on the scattering angle resolution ( $\sim 0.1 \mu\text{rad}$ ) which is dominated by multiple scattering.

The measurement of the *micro-beam* dispersion at the crystal position can

be made with the downstream tracker with the same angular resolution as for the exit angle determination ( $2.5 \mu\text{rad}$ ). The resolution is not improved by the presence of the upstream silicon detectors. The measurement resolutions and the corresponding *micro-beam* dispersions at the crystal position for different upstream detector combinations are listed in table 2.

## Conclusions

The performance of silicon microstrip detectors for the Crystal Experiment in the H8 beam line of the CERN SPS has been studied in order to establish a realistic scenario for the September 2006 test beam. The study is based on the performance of tested silicon detectors (AMS-02) and detectors whose performance can be reasonably well predicted (IRST).

For the scattering angle, a *micro-beam* with a  $3 \mu\text{rad}$  (rms) dispersion at the bent crystal position and a downstream silicon tracker with a 35 m flight path (in vacuum) will provide a measurement resolution of  $4.0 \mu\text{rad}$ . A comparable resolution ( $4.4 \mu\text{rad}$ ), with an event-by-event measurement of the incident beam angle, can be achieved with an upstream tracker composed of the better resolution IRST detectors and a 4.1 m flight path. The presence of the upstream tracker would determine the position of the incident protons at the crystal with a precision of  $8 \mu\text{m}$ .

For the *micro-beam* measurement, the downstream silicon tracker will provide a measurement resolution of  $2.5 \mu\text{rad}$ . The resolution of the measurement is not affected by the presence of an upstream tracker, however the *micro-beam* dispersion would increase by 15-33%.

## Comments

*A priori*, the presence of the dipole fields around the crystal position are incompatible with an optimal performance of the silicon tracker(s). Similarly, it would be preferable to avoid placing trigger counters between the silicon detectors and the crystal. The instrumentation present 6 m downstream of the crystal position should be replaced by vacuum as proposed.

Given the high level of precision required, the effects due to multiple scattering and finite detector resolutions should be taken into account in a Monte Carlo type analysis. In this perspective, the resolution of the new

IRST detectors must be measured, perhaps at least one IRST detector can be placed in the downstream telescope.

To exploit optimally the resolution of the silicon, the tracker alignment needs to determine the angles between the orientations of the  $xy$  planes of the different detectors, which implies a beam divergence comparable to the range of the scattered angle distribution,  $100\ \mu\text{rad}$  at the downstream telescope.

Since the presence of a  $3.0\ \mu\text{rad}$  *micro-beam* at the crystal position implies a smaller dispersion upstream of the crystal (fig. 4), the installation of a vacuum in place of the instrumentation located before the upstream dipole magnet, at 4.4 m from the crystal position, would improve the measurement. With the additional length in vacuum, and the suppression of two mylar windows, the *micro-beam* dispersion at the crystal would be  $2.3\ \mu\text{rad}$ , and the scattering angle resolution obtained with the downstream tracker  $3.5\ \mu\text{rad}$  (table 1).

Table 1: The angular resolutions of the upstream and downstream trackers and the corresponding scattering angle resolutions for the two upstream configurations and with the *micro-beam*, i.e. without the upstream telescope. The quoted resolutions refer to the root-mean-square (rms) of the distributions. The exit angle is determined with the combination S4-S5-S6. The question of a  $2.3 \mu\text{rad}$  *micro-beam* is raised in the **Comments**.

upstream configuration	$\Delta\theta_{\text{inc}}$ ( $\mu\text{rad}$ )	$\Delta\theta_{\text{exit}}$ ( $\mu\text{rad}$ )	$\Delta\theta_{\text{scat}}$ ( $\mu\text{rad}$ )
S1-S3	6.12	2.49	6.63
S1-S2-S3	5.46	2.49	6.03
with $7.5 \mu\text{m}$ resolution for S1-S2-S3			
S1-S3	3.79	2.49	4.59
S1-S2-S3	3.52	2.49	4.36
with $3.0 \mu\text{rad}$ <i>micro-beam</i>			
-	3.00	2.47	4.01
with $2.3 \mu\text{rad}$ <i>micro-beam</i>			
-	2.32	2.47	3.52

Table 2: *Micro-beam* dispersion at the crystal position and the corresponding dispersion measurement resolution for different silicon detector configurations (crystal removed, the quoted detectors and the downstream telescope S5-S6-S7-S8 in place).

upstream configuration	$\Theta_{inc}$ ( $\mu\text{rad}$ )	$\Delta\Theta_{inc}$ ( $\mu\text{rad}$ )
S4	3.01	2.46
S1-S4	3.57	2.32
S3-S4	3.52	2.39
S1-S3-S4	4.06	2.51
S1-S2-S3-S4	4.42	2.47

### H8 beam line

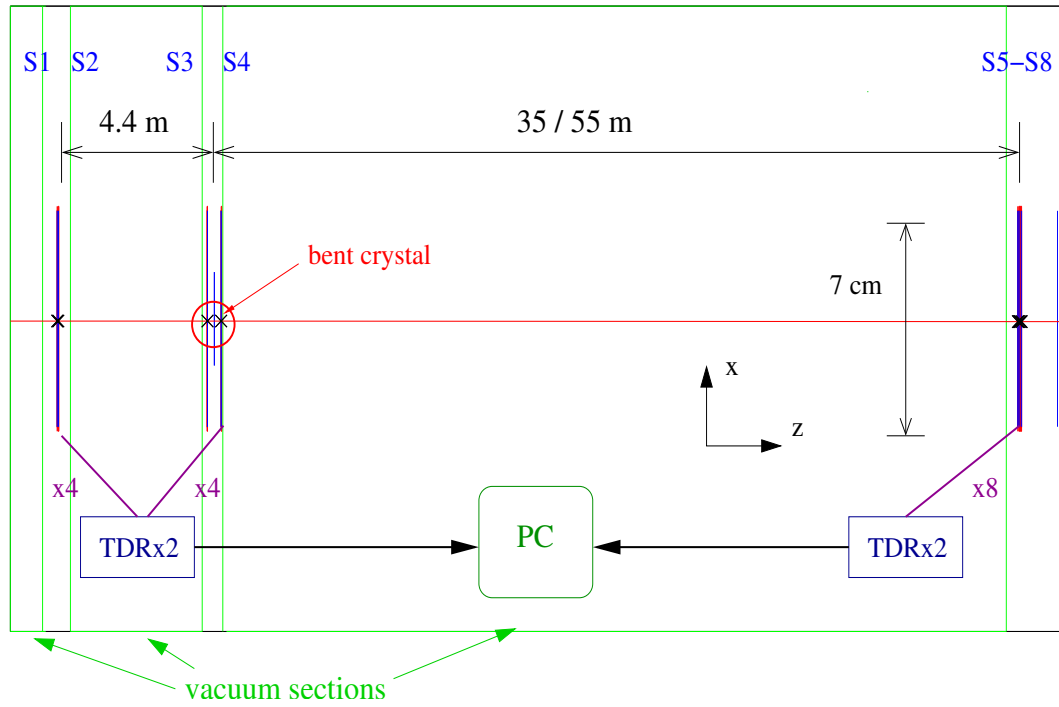


Figure 1: Positions of the silicon microstrip detectors (S1-S8) in the H8 beam line.



### Upstream Silicon Tracker in H8 beam line

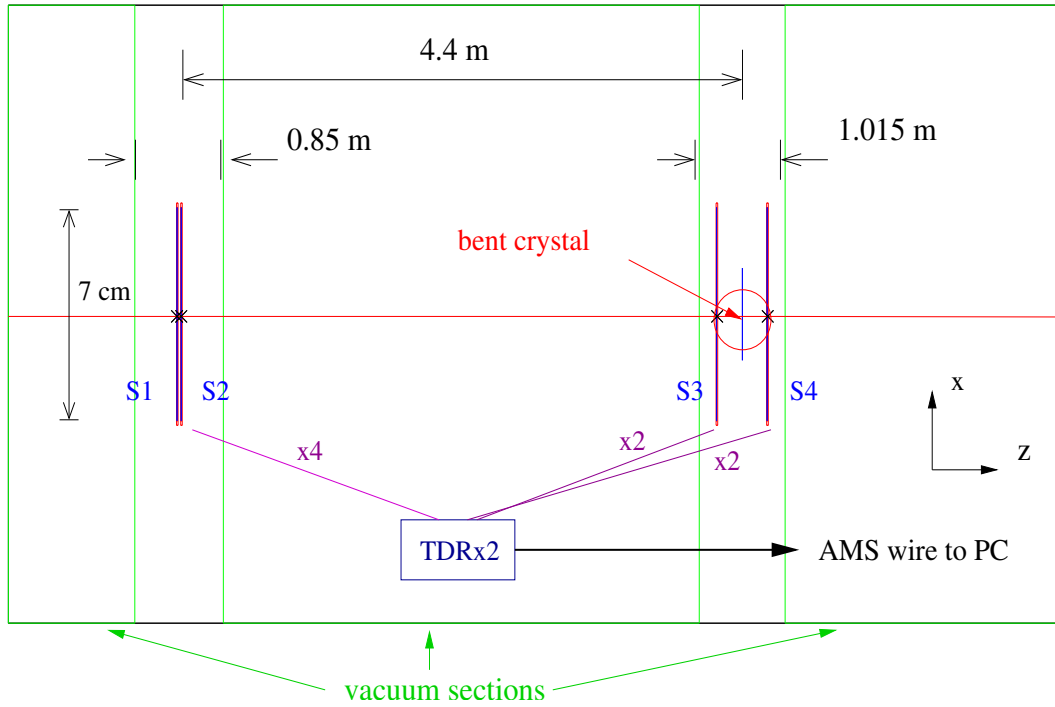


Figure 2: The silicon detectors (S1-S4) located upstream and around the bent crystal position.

### Downstream Silicon Telescope

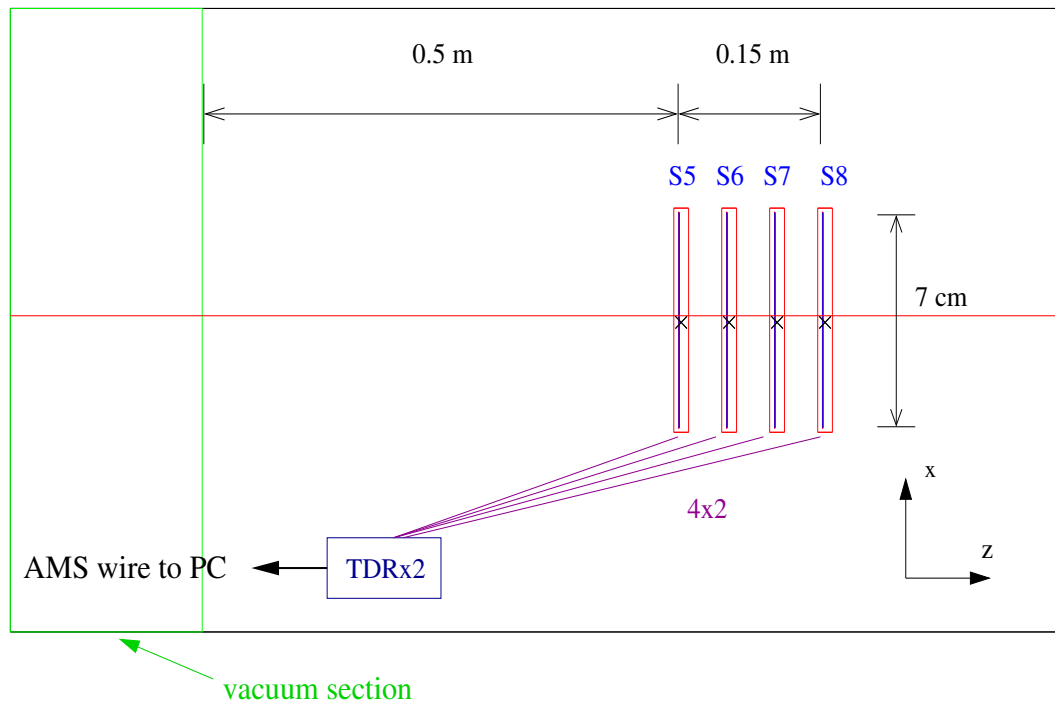


Figure 3: The silicon detectors (S5-S8) of the downstream telescope.

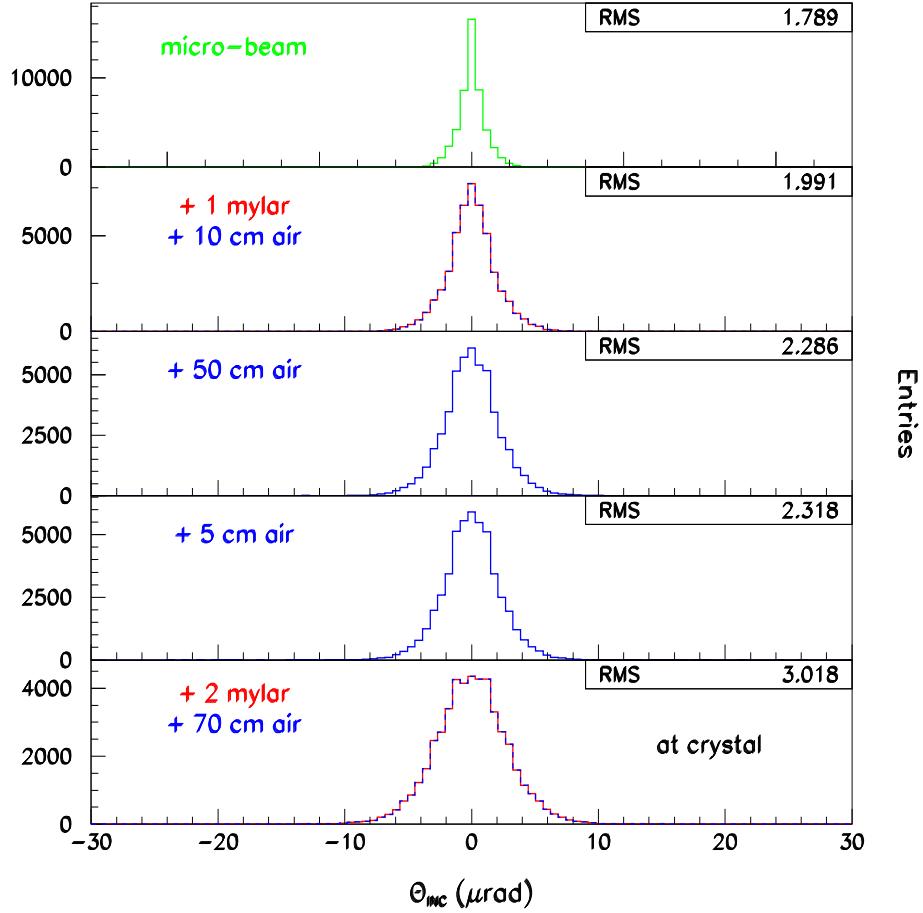


Figure 4: Evolution of the simulated beam dispersion from the generated position in the first vacuum section to the crystal position (fig 2). The material traversed since the preceding position is indicated (the silicon detectors of the upstream tracker are not present).

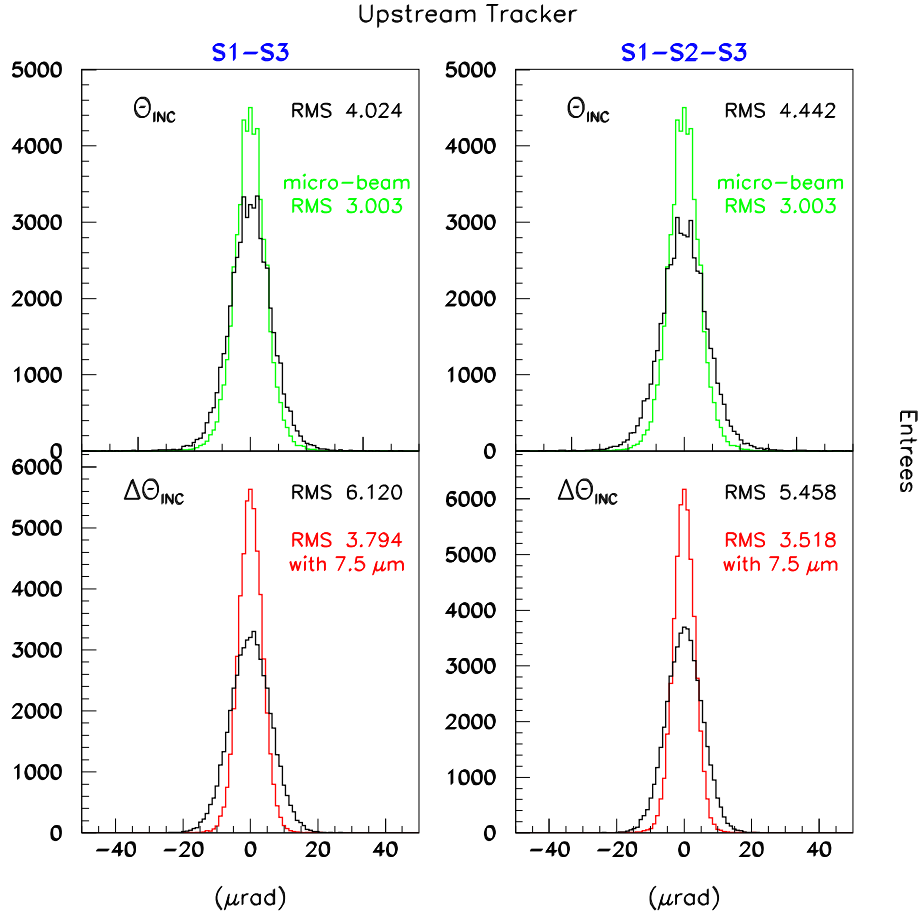


Figure 5: Upstream tracker performance with two (left) and three (right) silicon detectors: angular distribution of the beam at the entry with and without the upstream silicon detectors (top), angular resolution of the upstream tracker and the resolution obtained with the better resolution ( $7.5 \mu\text{m}$ ) IRST detectors (bottom).

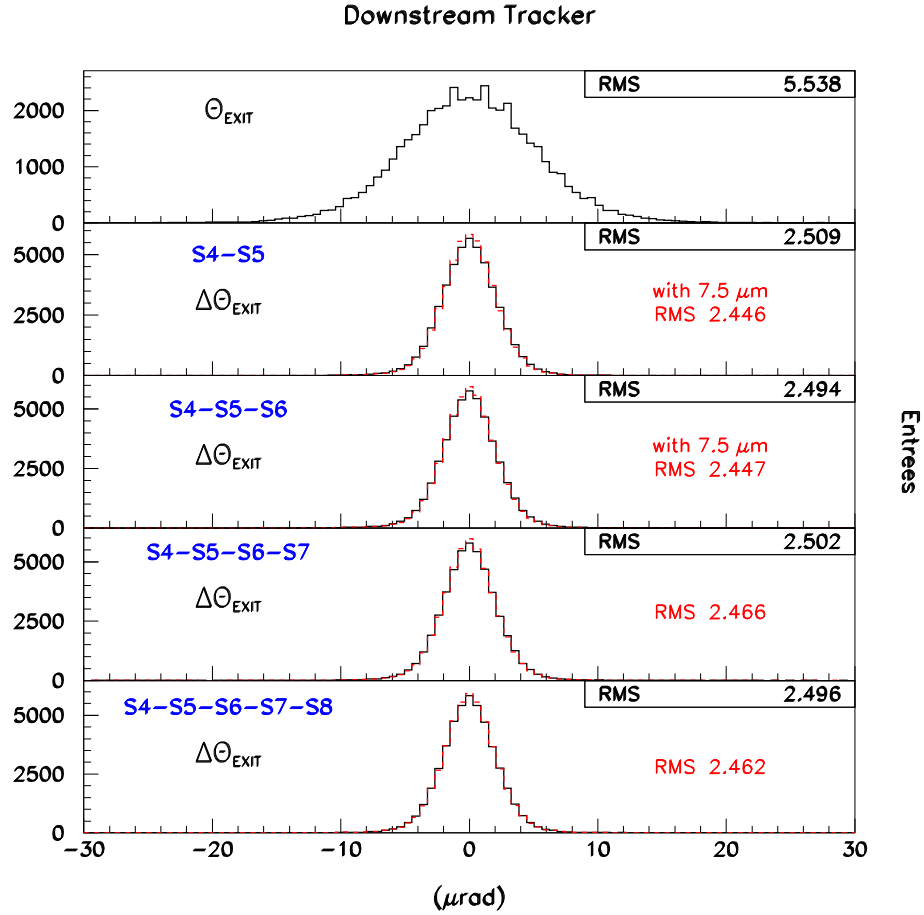


Figure 6: Downstream tracker performance: angular distribution of the scattered beam at the exit of the crystal (top), and the angular resolutions corresponding to different combinations of the silicon detectors of the downstream telescope, as well as the results obtained with the better resolution (7.5  $\mu\text{m}$ ) IRST detectors at the positions S4, S5, and S6.

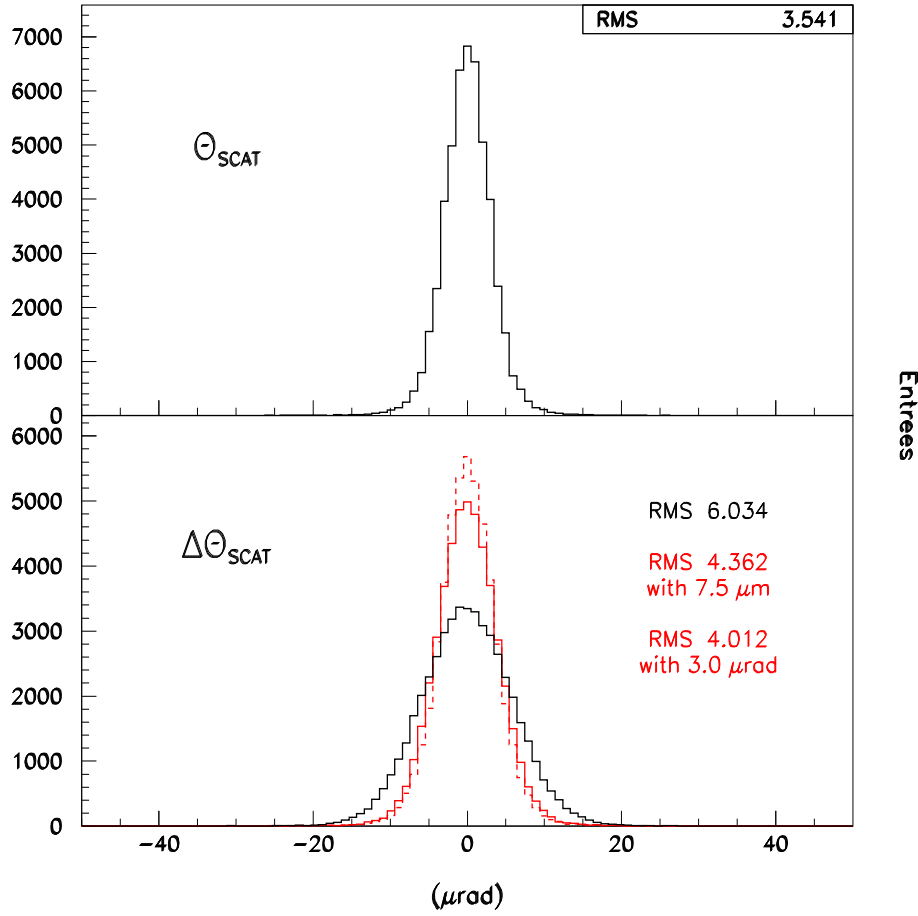


Figure 7: The scattered angle ( $\Theta_{\text{exit}} - \Theta_{\text{inc}}$ ) distribution (top) and the scattered angle resolutions obtained with the three-detector-upstream tracker equipped with AMS-02 detectors ( $15 \mu\text{m}$ ) and the better resolution ( $7.5 \mu\text{m}$ ) IRST detectors (bottom). The angular resolution obtained with only the downstream telescope and the *micro-beam* with a  $3 \mu\text{rad}$  (rms) dispersion at the crystal is also shown (dashed line). The observed deflection is due to multiple scattering in the 1 mm thick silicon wafer placed at the crystal position.

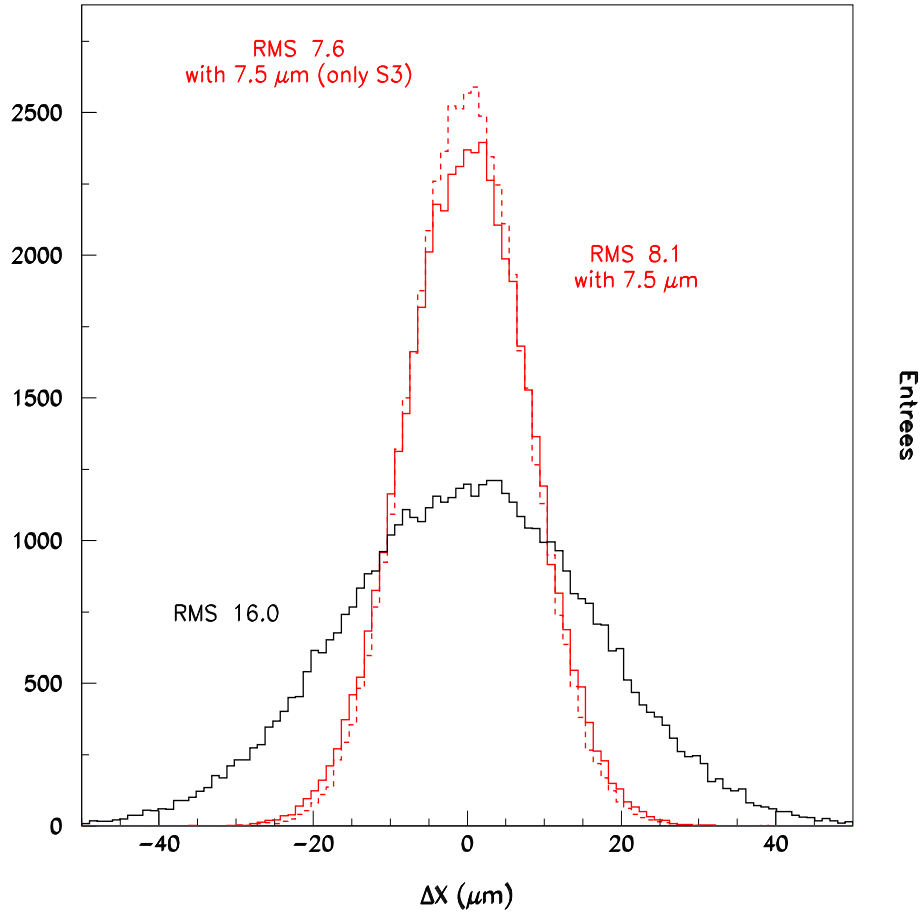


Figure 8: The precision of the predicted  $x$  position at the entry of the crystal provided with the upstream tracker equipped with the AMS-02 ( $15 \mu\text{m}$ ) or IRST ( $7.5 \mu\text{m}$ ) detectors. The results are identical for the two and three detector configurations. A single IRST detector at the position of S3 provides a comparable precision (dashed line).